Advantages of an InGaN-based light emitting diode with a p-InGaN/p-GaN superlattice hole accumulation layer

Liu Chao(刘 超), Ren Zhi-Wei(任志伟), Chen Xin(陈 鑫), Zhao Bi-Jun(赵璧君), Wang Xing-Fu(王幸福), Yin Yi-An(尹以安), and Li Shu-Ti(李述体)†

Institute of Opto-electronic Materials and Technology, South China Normal University, Guangzhou 510631, *China*

(Received 25 October 2012; revised manuscript received 2 February 2013)

P-InGaN/p-GaN superlattices (SLs) are developed for a hole accumulation layer (HAL) of a blue light emitting diode (LED). Free hole concentration as high as 2.6×10^{18} cm^{-3} is achieved by adjusting the Cp_2Mg flow rate during the growth of p-InGaN/p-GaN SLs. The p-InGaN/p-GaN SLs with appropriate Cp_2Mg flow rates are then incorporated between the multi-quantum well and AlGaN electron blocking layer as an HAL, which leads to the enhancement of light output power by 29% at 200 mA, compared with the traditional LED without such SL HAL. Meanwhile, the efficiency droop is also effectively alleviated in the LED with the SL HAL. The improved performance is attributed to the increased hole injection efficiency, and the reduced electron leakage by inserting the p-type SL HAL.

Keywords: light emitting diodes, hole accumulation layer, efficiency droop

PACS: 85.60.Jb, 78.60.Fi, 73.61.Ey **DOI:** 10.1088/1674-1056/22/5/058502

1. Introduction

The performance of the light emitting diode (LED) has experienced rapid progress in recent years. Nevertheless, there still remain some critical problems preventing LEDs from broader applications. One major obstacle for LEDs to overcome to penetrate into the general illumination market is the relatively low luminous efficiency. More remarkably, when it comes to the high injection current situation, the emission efficiency will experience sharp decline, referred to as "efficiency droop", which will hinder further application in high power lighting. Several causes for this effect have been reported in recent publications, such as Auger scattering,[1] carrier delocalization,[2] restricted hole injection,[3,4] and electron leakage.[5,6] It is commonly accepted that the effective mass of holes in GaN is large, while the mobility of holes is low, leading to insufficient hole injection into the active region. Moreover, the electron has a small effective mass and relatively high mobility, which makes it easy for it to overflow the quantum barriers into the p-type region, lowering the luminance efficiency. Furthermore, the lattice mismatch between the last GaN barrier and AlGaN electron blocking layer (EBL) will result in severe piezoelectric polarization at the GaN/AlGaN interface. The piezoelectric polarization field will lead to downward bending of the energy band of AlGaN EBL, which will also lower the capability of electron confinement and prevent efficient hole injection into the active region.

Many research groups have devoted their effort to the engineering of GaN-based LED epitaxial structures, which is thought to play a vital role in the alleviation of efficiency droop. By properly designing the p-type region structure, especially at the last GaN barrier/AlGaN EBL interface, the hole injection can be efficiently promoted and the electron leakage can be effectively inhibited.[7–9] Recently, modified EBL structures have been shown to improve the performance of LED, including elimination of the AlGaN EBL,[10] adoption of AlGaInN lattice matched EBL,[11] and replacement of AlGaN EBL with AlGaN/GaN/InGaN superlattices (SLs).[12] In our previous work, p-InGaN and p-AlGaN layers were inserted at the GaN/AlGaN interface to enhance the luminance efficiency and alleviate efficiency droop.[13,14] We have also experimentally demonstrated that InGaN/GaN superlattice can be used as a contact layer to lower the forward voltage and enhance the light output power, owing to the higher hole concentration in InGaN/GaN SL.[15] In view of the higher free hole concentration in InGaN/GaN SLs, we insert a p-InGaN/p-GaN SL hole accumulation layer (HAL) between multi quantum well (MQW) and EBL, in order to promote hole injection without lowering the capability of electron confinement.

2. Device structures and fabrication

Epitaxial structures of p-InGaN/p-GaN SLs and blue LEDs were grown by metal organic chemical vapour deposition (MOCVD) on *c*-plane sapphire substrates. The SL structures were mainly composed of 50 periods of p-$In_{0.05}Ga_{0.95}N$/p-GaN (2 nm/2 nm) SLs grown on a lightly Mg-doped GaN layer with high resistance. For the adjustment of Mg doping amount, three samples (labeled as sample I, II, and III) were grown with the same structures except for the Cp_2Mg flow rates during the growth of SLs, as shown in Table 1. The p-InGaN/p-GaN SL structure with appropriate Mg doping amount was then employed in the blue

†Corresponding author. E-mail: lishuti@scnu.edu.cn

© 2013 Chinese Physical Society and IOP Publishing Ltd

LED structure as hole accumulation layers. The original LED structure (labeled as sample A) was composed of a 25-nm-thick low-temperature GaN nucleation layer, a 2.0-μm-thick undoped GaN layer, a 2.0-μm-thick Si-doped GaN layer, 6-period $In_{0.16}Ga_{0.84}N$/GaN MQWs with 3-nm-thick wells and 10-nm-thick barriers, a 20-nm-thick p-$Al_{0.15}Ga_{0.85}N$ EBL, and a 170-nm-thick p-GaN layer. Another LED structure (labeled as sample B) is the same structure except that an 8-period p-$In_{0.05}Ga_{0.95}N$/p-GaN SL HAL was grown at 760 °C between the MQW and p-$Al_{0.15}Ga_{0.85}N$ EBL. The widths of the SL wells and barriers were both 2 nm. The Cp_2Mg flow rates were 360 sccm for InGaN wells and 120 sccm for GaN barriers during the growth of InGaN/GaN SLs. Subsequently, the SL structures were prepared for van der Pauw Hall measurements to examine the free hole concentration. The LED chips with a mesa size of 300 μm×300 μm were fabricated using a conventional mesa structure method, and processed into capsulated LEDs. The electrical properties were measured by on-wafer probing. The luminescence properties were collected by a calibrated integrating sphere with pulse mode current at room temperature.

3. Results and discussion

The influences of Cp_2Mg flow rate on the electrical performance of p-InGaN/p-GaN SLs are listed in Table 1. When the Cp_2Mg flow rates are 180 sccm for InGaN and 60 sccm for GaN in sample I, the hole concentration in the p-type SLs is 8.2×10^{17} cm^{-3}. The highest hole concentration (2.6×10^{18} cm^{-3}) is achieved in sample II when Cp_2Mg flow rates increase to 360 sccm and 120 sccm for InGaN wells and GaN barriers, respectively. As the Cp_2Mg flow rates further increase to 720 sccm or 240 sccm for InGaN or GaN SLs, the hole concentration declines to 6.8×10^{17} cm^{-3}. It is generally accepted that a deep donor level will be formed when Mg dopant concentration is high enough. As a result, the hole concentration will experience a decline with the further increase of the Cp_2Mg flow rate. The results indicate that the optimum values for Cp_2Mg flow rates are 360 sccm for InGaN wells and 120 sccm for GaN barriers. Therefore, the Cp_2Mg flow rates of 360 sccm or 120 sccm for InGaN or GaN SLs have been adopted during the growth of the p-InGaN/p-GaN hole accumulation layer.

Table 1. Influences of Cp_2Mg flow rate on hole concentration of InGaN/GaN SLs.

	R for InGaN/sccm	*R* for GaN/sccm	Hole concentration/cm^{-3}	Hole mobility/$cm^2\cdot V^{-1}\cdot s^{-1}$
Sample I	180	60	8.2×10^{17}	18.2
Sample II	360	120	2.6×10^{18}	12.5
Sample III	720	240	6.8×10^{17}	9.5

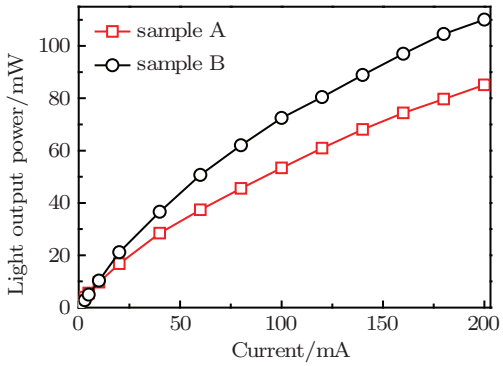


Fig. 1. (color online) Plots of light output intensity versus injection current for the two samples.

The forward voltages at 20 mA of samples A and B are 3.18 and 3.23 V, respectively, indicating that the forward voltage does not change much after the p-InGaN/p-GaN SL HAL has been inserted. The measured light–current (L–*I*) performances of the two samples with the increase of injection currents are shown in Fig. 1. The light output intensity increases sublinearly in both samples, owing to the efficiency droop effect. However, the variation trends of the two L–*I* curves differ from each other. At low injection current (below 6 mA), the light output intensity of sample A is larger than that of sample B. With the injection current further increasing, the light output intensity of sample A is surpassed by that of sample B. At an injection current of 200 mA, the light output intensity of sample B is 29% larger than that of sample A, which indicates that the introduction of p-InGaN/p-GaN SL HAL will enhance the light output intensity. Moreover, it is worth noting that the downward bending of the L–*I* curve in sample B is not as severe as that in sample A due to mitigated efficiency droop, which reveals that the adoption of p-InGaN/p-GaN SL HAL also helps to alleviate the efficiency droop.

The peak wavelengths and full widths at half maximum (FWHM) of the electroluminescence (EL) spectrum as functions of injection current for the two samples are plotted in Fig. 2. It is illustrated that the blueshift of peak wavelength in sample B (6.9 nm) is smaller than that in sample A (9.9 nm) as the injection current increases from 1 mA to 200 mA. Generally, the emission energy shifts can be explained by the Coulomb screening of the quantum confined stark effect and band-filling effect of carriers in QWs.[16] In our opinion, smaller lattice mismatch between the $In_{0.16}Ga_{0.84}N$/GaN MQWs and the $In_{0.05}Ga_{0.95}N$/GaN SL HAL in sample B will alleviate the polarization fields in MQWs, which should be

the main reason for the reduced blueshift of peak wavelength as the injection current increases. Besides, the FWHMs of the EL spectrums under small injection current remain almost the same in the two samples. However, with the injection current increasing from 1 to 200 mA, small broadening of FWHM is observed in sample B (7.9 nm), compared with that in sample A (10 nm). The broadening of FWHM is commonly attributed to the band filling effects in MQWs and self-heating effect. The lower growth temperature of $In_{0.05}Ga_{0.95}N$/GaN HAL (760 °C) in sample B will result in improved crystal quality in the MQW region, and consequently reduced broadening of FWHM in the LED with SL HAL.

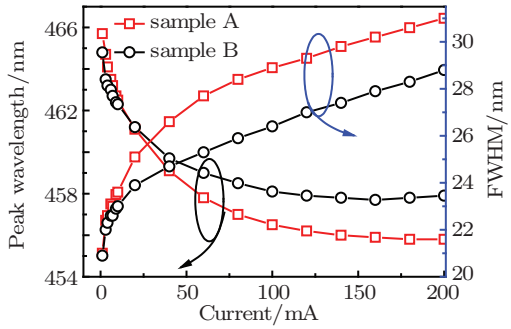


Fig. 2. (color online) Curves of peak wavelength and FWHM of EL spectrum versus injection current for the two samples.

In order to explain the improved performance in the LED with p-$In_{0.05}Ga_{0.95}N$/p-GaN SL HAL, the electrostatic fields, energy band diagrams, and the carrier distributions are simulated using the APSYS simulation software. The simulation structures are kept the same as our experimental samples. In the simulation, the built-in interface charges due to spontaneous and piezoelectric polarization are calculated using the methods developed by Fiorentini *et al.*[17] Considering the screening effect caused by defects, the polarization charge densities are assumed to be 50% of the calculated values. The Shockley–Read–Hall (SRH) lifetime is set to be 100 ns. The auger recombination coefficient is estimated to be of the order of 10^{-31} $cm^{-6}{\cdot}s^{-1}$. Most of the parameters used in this paper are the same as those in Refs. [18] and [19]. Other material parameters of the semiconductors used in the simulation can be found in Ref. [20].

Figure 3 shows the enlarged band diagrams near the EBL of the two samples. It is shown in sample A that the conduction and valence bands of the last barrier are severely bent, owing to the polarization field at the last barrier/AlGaN EBL interface, which will lead to electron leakage into the p-type region and insufficient hole injection into the active region. When the p-InGaN/p-GaN SLs are used, less band bending is observed, owing to a smaller lattice. Thus, more efficient electron confinement and hole transportation can be anticipated in the LED with SL HAL. Besides, the insertion of p-InGaN/p-InGaN SL HAL also results in more effective electron blocking and more efficient hole injection by AlGaN EBL. Specifically, as for sample A, the effective potential height for electrons in conduction band of EBL is 189.3 meV, and is 297.1 meV for sample B. On the other hand, the effective potential height for holes in the valence band of EBL in sample A is 230.7 meV, and is 201.5 meV for sample B. The increased effective potential height in the conduction band and the decreased effective potential height in the valence band indicate more effective electron blocking and hole injection, thereby enhancing the light output power and mitigating the efficiency droop.

Furthermore, it is worth noting that the InGaN/GaN SL HAL introduces a series of potential wells, thereby causing hole accumulation in the wells. At low injection current, holes are captured and confined in the wells of HAL. As a result, the light output power of sample B is smaller than that of sample A. However, in the high injection current condition, the hole accumulation will lead to much larger hole concentration, more efficient hole injection, and enhanced light output power.

Figure 4(a) shows the calculated electron distributions in the two samples at an injection current of 200 mA. Less electron leakage into the p-type region is seen in sample B (10^{13} cm^{-3}) than in sample A (10^{15} cm^{-3}). The electrons escaping into the p-type region will experience non-radiative recombination with the holes, thus lowering the luminance efficiency. Therefore, the reduced electron leakage will explain the higher internal quantum efficiency (IQE) as well as mitigated droop effects at 200 mA in the LED with SL HAL.

Figure 4(b) illustrates the hole concentration distributions in the two samples at 200 mA forward current. As for sample A, the hole concentration declines sharply through the EBL to a rather low level of 10^{15} cm^{-3} at the MQW/EBL interface, which will give rise to insufficient hole injection. As for sample B, the hole accumulation by the InGaN/GaN SL HAL will lead to gradually increasing hole concentration along the hole injection direction through the SL HAL. It is worth noting that the hole concentration in those periods of SL HAL adjacent to the MQW region is approximately at the level of 10^{18} cm^{-3}, much larger than that at the MQW/EBL interface of sample A (10^{16} cm^{-3}). Thus, more efficient hole injection into the active region is anticipated. As shown in the insert of Fig. 4(b), the hole concentration in the last quantum well is remarkably increased from 3.0×10^{19} cm^{-3} in sample A to 4.3×10^{19} cm^{-3} in sample B, which further confirms more efficient hole injection into the active region in the sample with SL HAL. Furthermore, electron concentration is also increased in the last few quantum wells adjacent to the p-type layer, owing to more

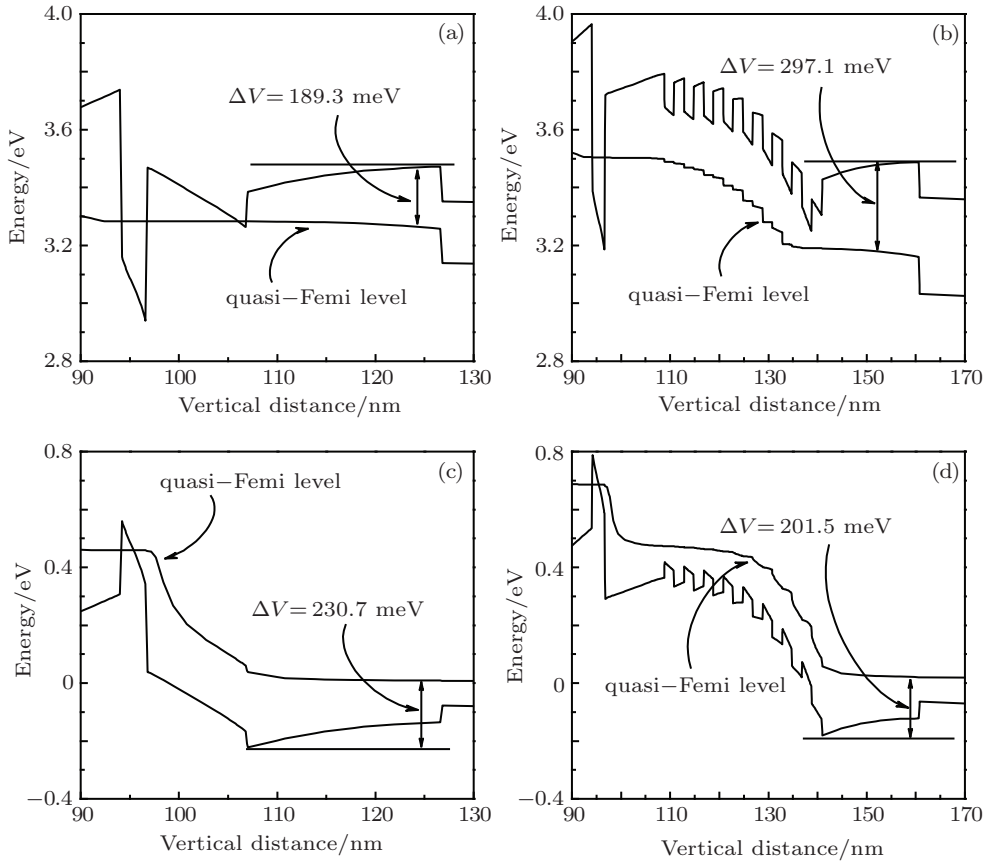


Fig. 3. Calculated conduction band diagrams of (a) sample A and (b) sample B; valence band diagrams of (c) sample A and (d) sample B at 200 mA forward current. The parameter ΔV represents the effective potential height for electrons.

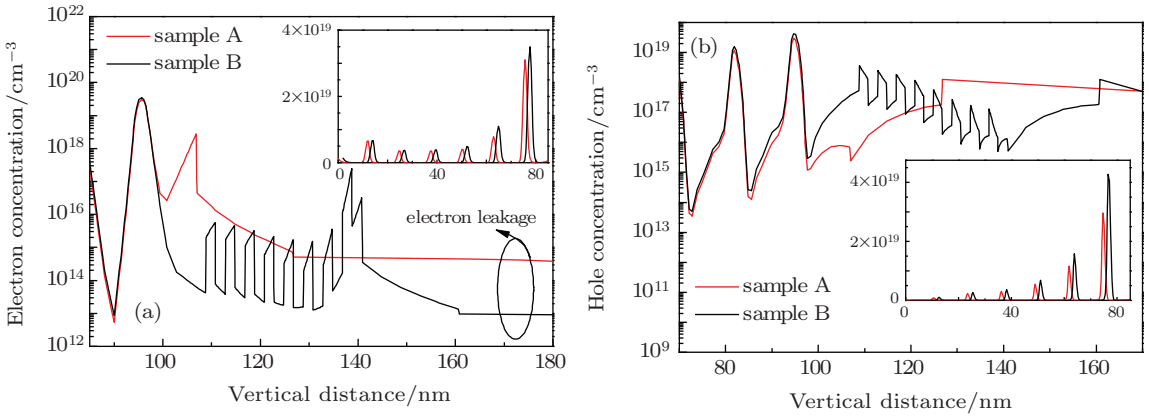


Fig. 4. (color online) (a) Electron concentration distributions in the two samples at 200 mA forward current. The insert shows electron concentration distributions in the active region. (b) Hole concentration distributions in the two samples at 200 mA forward current. The inset shows hole concentration distributions in the active region.

efficient electron confinement as shown in the insert of Fig. 4(a). David *et al.*[21] reported that the carriers were non-uniformly distributed in MQWs and only these wells adjacent to the p-type layer contributed to radiative recombination in LEDs. Hence, the increased electron and hole concentration in the last few wells will explain the increase of light output intensity in the LED with InGaN/GaN SL HAL.

Figure 5(a) illustrates the dependencies of calculated IQE on the injection current for the two samples. The IQE of sample B is improved remarkably compared with that of sample A. At an injection current of 200 mA, the internal efficiency is enhanced from 50.5% in sample A to 64.9% in sample B. Additionally, the efficiency droop, defined as $(\eta_{\text{peak}}-\eta_{200\text{ mA}})/\eta_{\text{peak}}$, is also alleviated from 45.7% in sample A to 28.5% in sample B. Figure 5(b) shows the curves of external quantum efficiency (EQE) as a function of injection current for the two samples. The experimental results also indicate that the droop of EQE is effectively mitigated in the sample with p-InGaN/p-GaN SL HAL. However, improvement in our experiment is not as significant as that in simulation, and is at-

tributed to the crystal quality that needs further optimization.

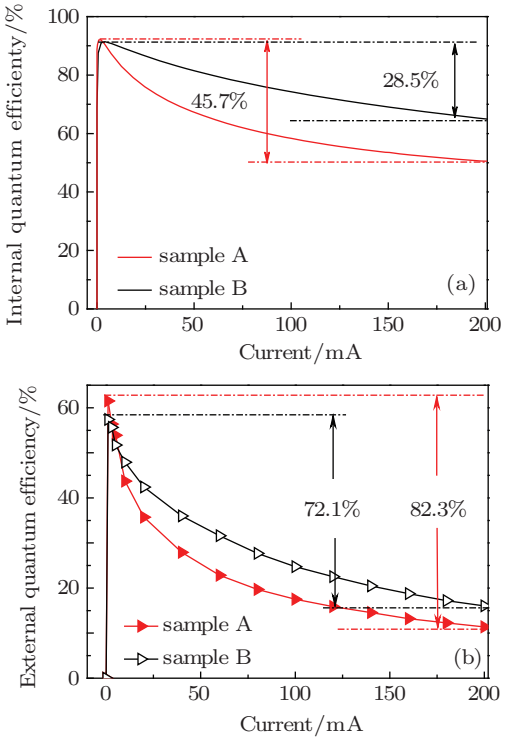


Fig. 5. (color online) (a) Simulated IQE and (b) calculated EQE as functions of the injection current for the two samples.

4. Conclusions

The influence of p-InGaN/p-GaN SLs on the performance of blue LEDs is investigated experimentally and numerically. The Cp_2Mg flow rates during the growth of the p-InGaN/p-GaN SLs are adjusted to achieve free hole concentration as high as 2.6×10^{18} cm^{-3}. The p-InGaN/p-GaN SLs with appropriate Cp_2Mg flow rates are then inserted in blue LEDs as HAL. The LED with SL HAL exhibits an enhanced light output power and a mitigated efficiency droop, compared with the traditional LED without SL HAL. It is mainly attributed to increased hole injection efficiency and decreased electron leakage.

References

[1] Shen Y C, Mueller G O, Watanabe S, Gardner N F, Munkholm A and Krames M R 2007 *Appl. Phys. Lett.* **91** 141101

[2] Monemar B and Sernelius B E 2007 *Appl. Phys. Lett.* **91** 181103

[3] Rozhansky I V and Zakheim D A 2007 *Phys. Stat Sol (a)* **204** 227

[4] Rozhansky I V and Zakheim D A 2006 *Phys. Stat Sol. (c)* **3** 2160

[5] Kim M H, Schubert M F, Dai Q, Kim J K, Schubert E F, Piprek J and Park Y 2007 *Appl. Phys. Lett.* **91** 183507

[6] Schubert M F, Xu J, Kim J K, Schubert E F, Kim M H, Yoon S, Lee S M, Sone C, Sakong T and Park Y 2008 *Appl. Phys. Lett.* **93** 041102

[7] Chen J, Fan G H and Zhang Y Y 2013 *Chin. Phys. B* **22** 018504

[8] Lu T P, Li S T, Zhang K, Liu C, Xiao G W, Zhou Y G, Zheng S W, Yin Y A, Wu L J, Wang H L and Yang X D 2011 *Chin. Phys. B* **20** 098503

[9] Wang T H and Xu J L 2012 *Chin. Phys. B* **21** 128504

[10] Han S H, Lee D Y, Lee S J, Cho C Y, Kwo M K, Lee S P, Noh D Y, Kim D J, Kim Y C and Park S J 2009 *Appl. Phys. Lett.* **94** 231123

[11] Kuo Y K, Tsai M C and Yen S H 2009 *Opt. Commun.* **282** 4252

[12] Kim K S, Kim J H, Jung S J, Park Y J and Cho S N 2010 *Appl. Phys. Lett.* **96** 091104

[13] Lu T P Li S T Liu C, Zhang K, Xu Y Q Tong J H Wu L J Wang H L Yang X D Yin Y A Xiao G W and Zhou Y G 2012 *Appl. Phys. Lett.* **100** 141106

[14] Wu L J, Li S T, Liu C, Lu T P, Xiao G W, Zhou Y G and Yin Y A 2012 *Chin. Phys. B* **21** 068506

[15] Li S T, Wu Q B, Fan G H, Zhou T M, Zhang Y, Yi Y A, He M, Cao J X and Su J 2009 *Semicond. Sci. Technol.* **24** 085016

[16] Chichibu S, Azuhata T, Sota T and Nakamura S 1996 *Appl. Phys. Lett.* **69** 4188

[17] Fiorentini V, Bernardini F and Ambacher O 2002 *Appl. Phys. Lett.* **80** 1204

[18] Xia C S, Li Z M, Lu W, Zhang Z H, Sheng Y, Hu W D and Cheng L W 2012 *J. Appl. Phys.* **111** 094503

[19] Xia C S, Hu W D, Wang C, Li Z F, Chen X S, Lu W, Li Z M and Li Z Q 2006 *Opt. Quantum Electron.* **38** 1077

[20] Vurgaftman I and Meyer J R 2003 *J. Appl. Phys.* **94** 3675

[21] David A, Grundmann M J, Kaeding J F, Gardner N F, Mihopoulos T G, Krames M R, Mihopoulos T G and Krames M R 2008 *Appl. Phys. Lett.* **92** 053502